JOURNAL OF CATALYSIS 71, 278–287 (1981)

Thermal Desorption Spectroscopy from High-Specific-Area Solids—Hydrocarbon Adsorption and Diffusion in NaX Zeolite Crystals

M. KISKINOVA,[1] G. L. GRIFFIN,[2] AND J. T. YATES, JR.

Surface Science Division, National Bureau of Standards, Washington, D.C. 20234

Received February 9, 1981; revised May 28, 1981

This work illustrates a novel application of the thermal desorption spectroscopy technique to investigate adsorption, desorption, and surface diffusion phenomena on small zeolite crystals. Ultrahigh-vacuum procedures employed with zeolite samples of very small mass permit measurements to be made without the presence of intergranular diffusion effects. Studies of 1-butene and C_2H_4 adsorption have been carried out. A diffusion energy of ~2.7 kcal/mole has been measured for 1-butene on zeolite-X; for C_2H_4 the measured diffusion energy is ~1.9 kcal/mole. The desorption energy for C_2H_4 on zeolite-X is kinetically measured to be 8.9 kcal/mole in excellent agreement with the isosteric heat of adsorption (8.9 kcal/mole). The characteristic behavior of adsorbate thermal desorption states upon annealing may be employed to discriminate between species adsorbed on the outer surface of the zeolite crystals, and species which are present within the pores of the zeolite.

I. INTRODUCTION

Thermal desorption spectroscopy (TDS) is widely applied to the study of adsorption/desorption phenomena on single-crystal substrates having surface areas of the order of 1 cm^2 (*1*). This type of measurement is usually carried out in an ultrahigh-vacuum system using mass spectrometric detection of desorbing species. Typically, desorption signals of the order of 10^{-8} Torr are measured above background pressures of the order of 10^{-10} Torr in vacuum systems having nominal pumping speeds of $\sim 10^5$ cm^3 s^{-1}.

In the last few years, TDS has also been applied to the study of desorption from high-area solids of catalytic interest (*2*). Generally, large quantities of the powdered solid are employed in the form of a packed bed whose temperature may be varied using a programmable heating source. While measurements of this kind are useful, they would not be expected to possess the well-defined character of desorption from single-crystal surfaces. Among the possible reasons for this are:

(1) adsorption site heterogeneity characteristic of high-area solids,

(2) intergranular diffusion processes through a packed bed,

(3) temperature gradients through the sample.

By employing ultrahigh-vacuum techniques we have shown that it is possible to do temperature-programmed desorption from high-specific-surface-area powders of very low mass presenting only several square centimeters of adsorbent surface area. Working with small samples in this regime, one can minimize or eliminate intergranular diffusion effects and thermal gradients, leading to a closer relation between the observed thermal desorption processes and elementary activated surface processes on the particles themselves.

Our first studies of adsorption/desorp-

[1] Guest Worker, NBS, 1980. Permanent address: Academy of Sciences of Bulgaria, Institute of General and Inorganic Chemistry, Sofia 13, Bulgaria.

[2] NRC Postdoctoral Research Associate, 1980. Permanent address: Department of Chemical Engineering and Materials Science, University of Minnesota, Minneapolis, Minnesota 55455.

0021-9517/81/100278-10$02.00/0

tion phenomena from high-specific-surface-area materials have employed small crystallites of a zeolite as an adsorption substrate for small hydrocarbon molecules. Zeolites have a well-defined alumino–silicate lattice structure with the possibility of producing an endless number of modifications by changing guest cations, composition, position, and number (*3–5*). These changes may strongly influence the binding energy of an adsorbate within the zeolite cages, thereby producing associated changes in catalytic activity and selectivity (*5, 6*). The conventional procedure for determining binding energies of adsorbates on zeolites involves the determination of isosteric heats of adsorption from adsorption isotherms (*3, 7*); this, however, is a time-consuming procedure carried out under *equilibrium* conditions. Recently, efforts to apply thermal desorption spectroscopy to bulk zeolite samples have been made (*8–10*) using gas chromatographic flow procedures to determine adsorbate binding energies. In those experiments, the influence of intergranular diffusion processes in the interstices (macropores) *between* zeolite crystals was undetermined.

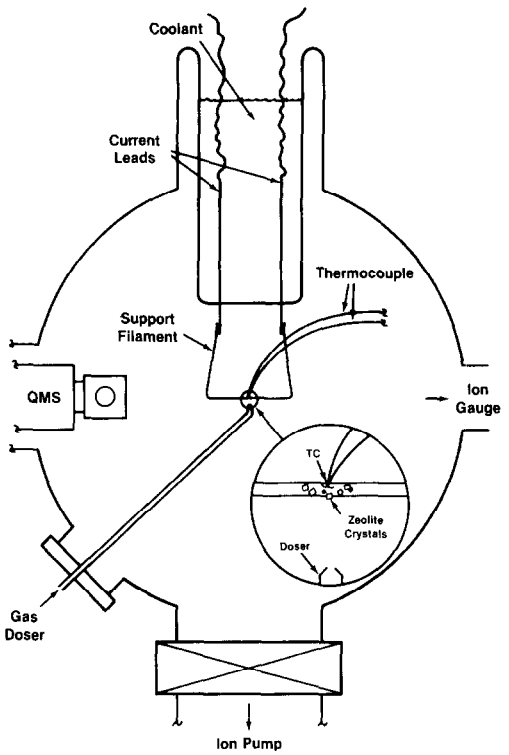

FIG. 1. Schematic of vacuum system for temperature-programmed desorption studies of zeolite single crystals.

The experiments to be reported here involve an exploratory investigation of olefin desorption from faujasite NaX crystals. Adsorption/desorption phenomena have been kinetically studied under *nonequilibrium* conditions. The primary goal was to determine what information can be obtained from temperature-programmed desorption procedures applied to very small crystals of the zeolite, which because of their combined small mass, are likely to be free from intergranular diffusion and thermal gradient effects. We are able to clearly resolve the relative contributions to the desorption spectra arising from diffusion *within* the zeolite particles and from desorption from the boundary of the zeolite crystals.

II. EXPERIMENTAL

The zeolite sample used was an unexchanged synthetic faujasite, NaX, donated by Union Carbide.[3] This is a large-pore zeolite, with a diameter of the apertures connecting supercages of about 8 Å. Both C_2H_4 and C_4H_8 adsorbates can easily pass through these apertures.

The experimental ultrahigh-vacuum apparatus is shown in Fig. 1. It consists of a stainless-steel vacuum chamber of 4×10^3 cm^3 volume connected to an ion pump of nominal 3×10^4 cm^3 s^{-1} pumping speed. The ion pump may be isolated from the chamber using an ultrahigh-vacuum gate valve of 10 cm internal diameter. The vacuum chamber contains a quadrupole mass spectrometer (QMS), a Bayard–Alpert ionization gauge for calibration of the QMS,

[3] We are indebted to Dr. J. A. Rabo of Union Carbide for providing zeolite crystals, and for helpful discussions.

and a gas doser inlet system. The zeolite sample is held on a tungsten support filament (diameter = 0.025 cm), to which is welded an Fe/constantan thermocouple. The tungsten support filament is welded to Ni feedthroughs which pass through a glass reentrant seal which forms a Dewar for thermostating the leads. Either cooled N_2 gas or liquid N_2 is used for cooling. Blank experiments to determine the influence of the tungsten filament as an adsorbent were done using a second control filament which did not contain the zeolite sample. In no cases was the desorption signal from the control filament greater than 1–2% of the signal from the zeolite-coated filament. Both of the tungsten filaments were in fact known to be coated with a layer of tungsten oxide (*11*) and may therefore be considered to be inactive catalytically in the experiments carried out here. The geometrical surface area of the support filament is small (~1 cm^2) compared to the zeolite sample's internal surface area (~500 cm^2).

The zeolite sample (~1-μm crystals) was deposited on the support filament as follows: A dilute slurry of zeolite and distilled H_2O was prepared. A small drop of this slurry was placed near the center of the filament, and the water was allowed to evaporate, leaving a coating of zeolite crystals along a ~0.3-cm length of the support filament. Following our experiments, the zeolite was washed off the weighed filament with H_2O, and the zeolite mass was determined to be $\gtrsim 6 \times 10^{-5}$ g by reweighing the filament. For adsorption experiments on the zeolite, the support filament assembly was loaded into the vacuum system. Bake-out at ~200°C yielded an ultimate vacuum of $< 1 \times 10^{-8}$ Torr. The zeolite sample was then heated to 400°C for a few minutes under vacuum and cooled down to the desired adsorption temperature. The system was isolated from the pump, the ionization gauge was turned off, and a finite pressure of the adsorbate gas was admitted to the static system using the QMS as a pressure monitor before it too was turned off. All exposures were made by varying the pressure of the adsorbate in the chamber rather than the time of adsorption. Following the desired exposure, the gate valve was opened and the gas was pumped away. Following a suitable delay time, the filament was electrically heated using an ac heating program at ~5 K $s^{-1} = \beta$, and the partial pressure of desorbing gas was recorded as a function of time using the QMS. The experiments shown here were repeated on separate zeolite preparations to assure that the basic qualitative features were reproducible.

III. RESULTS

A. 1-Butene Adsorption

Our initial experiments were performed with 1-butene. Figure 2 shows the C_4H_8 (m/e = 56) desorption spectra following successively greater exposure to 1-butene. Exposures are reported in Langmuirs, L, where 1 L = 10^{-6} Torr s. For all of these experiments, a fixed delay time of 120 s was employed for pumping away the C_4H_8 (g) prior to initiating the temperature-programmed desorption. The amount of adsorbate determined from the area under the

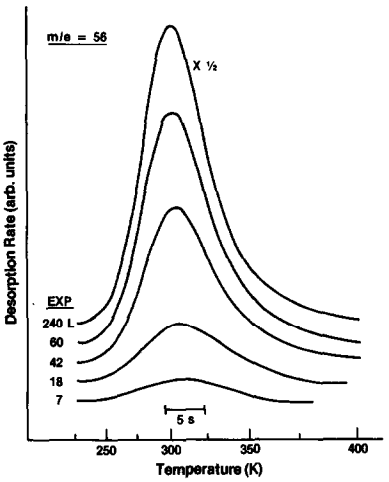

FIG. 2. Thermal desorption spectra of 1-butene on zeolite NaX, for various exposures. (Exposures given in Langmuirs; 1 L = 10^{-6} Torr; exposure temperature = 225 K.)

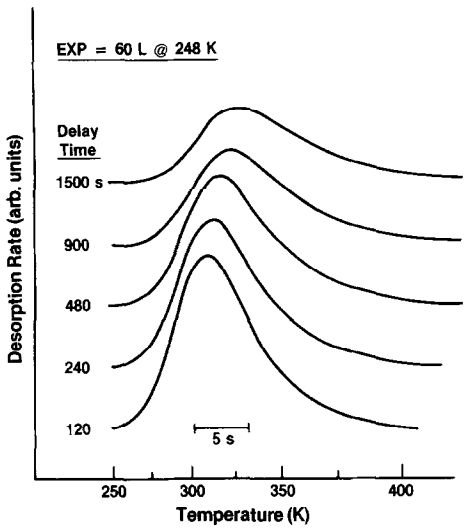

FIG. 3. Thermal desorption spectra of 1-butene on zeolite NaX, for various delay times before starting temperature programming.

desorption curves increases linearly with exposure up to 60 L exposure. As the coverage on the zeolite is increased over the range shown in Fig. 2, a ~7 K decrease in the peak temperature is observed.

A series of thermal desorption experiments was performed in which various delay periods at 248 K were employed following a 60-L exposure to 1-butene. The results are shown in Fig. 3 for delay times from 120–1500 s. Two effects are observed as delay time was increased:

(1) The desorption peak maximum shifts to higher temperature.

(2) The area under the desorption peak and hence the amount of adsorbate decreases.

In order to be certain that the shift of the desorption peak to higher temperature was an effect related to delay time and not to amount of 1-butene present on the zeolite, the experiment in Fig. 4 was carried out. Here the two solid desorption curves correspond to a 60-L exposure with delay times of 120 and 1500 s. The dashed desorption trace corresponds to a 30-L exposure followed by a 120-s delay. The areas under the top two curves are identical indicating that the shift to higher temperature is directly related to the delay time employed and not to the quantity of 1-butene present. On the basis of these experiments, we conclude that the peak shift to higher temperatures is related to the diffusion of 1-butene into the zeolite pores; the decrease in surface coverage associated with increased delay time under vacuum is due to desorption from the crystal boundary during the delay period at 248 K.

It is instructive to examine a plot of desorption peak temperatures versus delay time at various sample temperatures as shown in Fig. 5. At the four experimental temperatures shown the peak temperature shift increases monotonically with delay time as shown. Furthermore, the magnitude of the observed peak temperature shift increases monotonically with sample temperature for all constant values of delay time. These observations suggest that the mean penetration depth of adsorbate into the zeolite pores increases with time and temperature, via an activated diffusion process. The experimental data obtained in this range of temperatures (225–283 K) and delay times (120–1500 s) show no tendency for reaching a maximum peak temperature. This suggests that full penetration of 1-

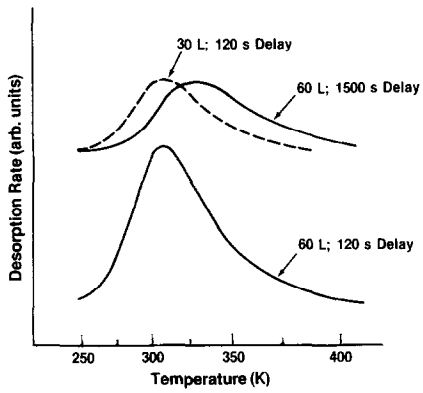

FIG. 4. Thermal desorption spectra of 1-butene on NaX. Effect of adsorbate penetration (exposure temperature = 250 K). Lower curve, exposure = 60 L, delay time = 120 s. Upper curve, solid line same as lower curve except delay time = 1500 s; dashed line same as lower curve, except exposure = 30 L.

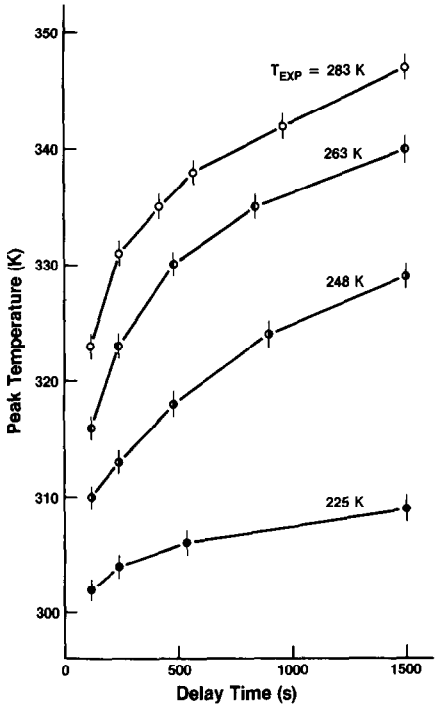

FIG. 5. Observed temperature maximum for 1-butene on zeolite NaX as a function of delay time before starting temperature programming for various temperatures.

butene into the zeolite crystallites has not occurred following the 1500-s diffusion experiment at 283 K.

By analyzing the decay curves representing the amount of adsorbate remaining as a function of delay time under vacuum, we can estimate the activation energy of the rate-limiting process for loss of adsorbate from the zeolite crystallites. In Fig. 6 is shown a plot of the amount of adsorbate as a function of delay time for experiments performed at various exposure temperatures. The data are not first order over the full range of delay times, as indicated by the curvature of the semilogarithmic plots. However, an empirical first-order decay constant may be defined from data taken from the first two points in each curve where linear behavior is nearly obeyed. The Arrhenius plot for these data is shown in Fig. 6b and an activation energy of ~2.7 kcal/mole is obtained. This energy is too low for a desorption energy and indicates that diffusion from the zeolite pores out to the zeolite crystal surface is the rate-limiting step in the process associated with loss of 1-butene during the delay period under vacuum. This observation suggests that when a 1-butene molecule diffuses to the surface at $T \geq 225$ K it desorbs immediately.

B. C_2H_4 Adsorption

To determine if thermal desorption spec-

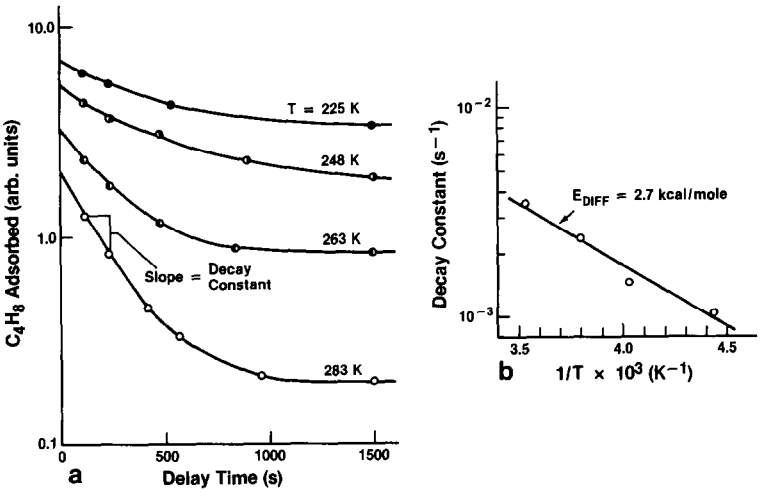

FIG. 6. Decay of adsorbate concentration during delay following exposure (1-butene on zeolite NaX). (a) Amount of 1-butene remaining prior to desorption, as a function of delay time before warm-up; (b) Arrhenius plot of empirical decay constants.

troscopy could provide information about adsorption energetics without undue interference from diffusion effects, a second set of experiments was performed using C_2H_4 as adsorbate at lower temperatures. In Fig. 7 are shown the desorption spectra for C_2H_4 desorbing from NaX for various exposures at 120 K. The delay time between the end of the exposure and the beginning of desorption was 120 s. Two features are resolved. There is a low-temperature state with peak maximum at ~150 K which is populated first (state 1). There is also a second higher-temperature desorption state with peak maximum at ~210 K which is populated at later stages and which dominates at higher exposures (state 2). As with 1-butene, the quantity of C_2H_4 adsorbed increases linearly with exposure and there is no indication of a saturation condition being reached at 750 L exposure.

Diffusion experiments were carried out at 120 K by varying the delay time under vacuum as shown in Fig. 8. The low-temperature peak decreases slightly in magnitude and shifts slightly to higher temperature as the delay time is increased, as was observed for 1-butene. However, the high-temperature binding state is unaffected by delays under vacuum suggesting that major diffusion effects are absent at 120 K for this species.

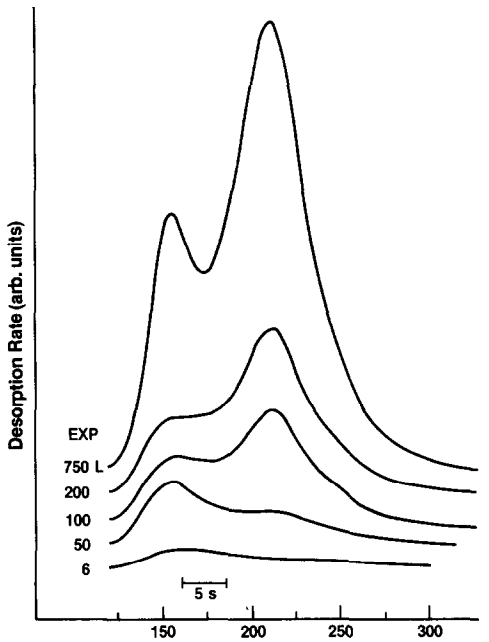

FIG. 7. Thermal desorption spectra of C_2H_4 on zeolite NaX, for various exposures. (Exposure temperature = 120 K.)

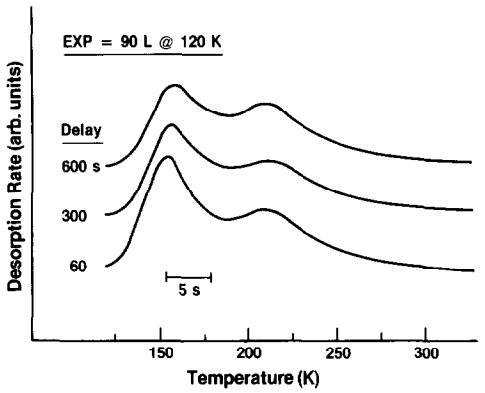

FIG. 8. Thermal desorption spectra of C_2H_4 on zeolite NaX for various delay times before starting warm-up. Negligible diffusion effects.

Experiments were also performed at higher temperatures, (190–250 K), where behavior would be expected to be similar to that observed for 1-butene. At 190 K, the low-temperature peak could no longer be populated, and the high-temperature binding state of C_2H_4 decreased in intensity and shifted upward in peak temperature with increasing delay time under vacuum in much the same manner as observed for 1-butene. Thus this state is also influenced at higher temperatures by diffusion into the zeolite pores. An Arrhenius plot of the decay constants, as described above for 1-butene, gave an activation energy for C_2H_4 diffusion of ~1.9 kcal/mole.

IV. DISCUSSION

A. Adsorbed Amounts and Sensitivity of TDS for High-Area Adsorbents

Barrer *et al.* (*3*) reported saturation amounts for C_2H_6 and C_4H_{10} on zeolite-X from their reversible isotherm measurements. We would expect similar amounts of

TABLE 1

Quantity of Hydrocarbon Adsorbed on Zeolite-X

Molecule	Saturation amount/g zeolite (mole)	Maximum amount/g zeolite this work (mole)	Percentage saturation
C_2H_6	3.6×10^{-3}	—	—
n-C_4H_{10}	2.2×10^{-3}	—	—
C_2H_4	$(3.6 \times 10^{-3})^a$	0.3×10^{-3}	$(8)^a$
1-C_4H_8	$(2.2 \times 10^{-3})^a$	0.02×10^{-3}	$(1)^a$

[a] Estimated values, based on saturation values reported in Ref. (*4*) for C_2H_6 and C_4H_{10}, assuming that these molecules are sterically similar to their olefin counterparts.

C_2H_4 and C_4H_8 to be adsorbed at saturation. In Table 1, a comparison is made between the two regimes of coverage employed at equilibrium and in this work. We see that our experiments always involved only partial filling of the zeolite pores with adsorbate.

The thermal desorption spectra shown in Figs. 2 and 7 show that the minimum measured quantities of adsorbate are a few percent of the maximum value obtained for 6×10^{-5} g of zeolite. Thus, a lower limit of detectability for a 6×10^{-5}-g sample of zeolite is roughly 10^{-3}–10^{-4} of the saturation value, corresponding to about 10^{12} desorbing species. Working with larger zeolite samples will of course increase the sensitivity of the method beyond that demonstrated here.

B. Energetics of Desorption and Diffusion

The systems C_2H_4/NaX and 1-butene/NaX were chosen for this exploratory study because information on the isosteric heats of adsorption has been obtained previously. Because of interference by diffusion into the zeolite pores, our experiments did not yield information on the kinetics of desorption of 1-butene from zeolite-X. For C_2H_4 at the lower temperatures, diffusion effects may be minimized and one may estimate the activation energy, E_d, for desorption from the TDS data, using the Redhead equation (*12*) for first-order desorption:

$$E/RT_m^2 = (\nu_0/\beta) \exp -E/RT_m. \quad (1)$$

Here T_m is the desorption peak temperature, β is the temperature scan rate (K/s), and ν_0 is the assumed first-order preexponential factor = 10^{13} s^{-1}. The observed desorption peaks at ~150 and ~210 K correspond to binding energies, E_d, of 8.9 and 12.6 kcal/mole, respectively. A comparison of these results with relevant literature data is shown in Table 2.

It may be seen from Table 2 that for C_2H_4, the lower activation energy for desorption (state 1) agrees fortuitously well with the isosteric heat measured by Bezus *et al.* (*4*). The origin of the higher-temperature desorption state (state 2) may be explained by various models:

1. State (2) could originate from C_2H_4 which has diffused into the pore structure of the zeolite via a weakly bound *second-*

TABLE 2

Desorption Energetics for Hydrocarbons on Zeolite-X

Molecule	Q_{st} (kcal/mole)	E_d (kcal/mole)	Reference
C_2H_6	6.2	—	(*4*)
n-C_4H_{10}	9.6	—	(*14*)
C_2H_4	8.9	8.9 (state 1) 12.6 (state 2)	(*4*); this work This work
1-C_4H_8	10.5	—	(*13*)

layer state which forms only when appreciable coverage has been achieved in the first (state 1) layer. In this model, diffusion at low temperatures is enhanced by adsorption of C_2H_4 on the outer surface of the zeolite, followed by migration into the pore. This model is consistent with the later development of state (2) compared to state (1).

2. State (2) could reflect the presence of a second binding state for C_2H_4 on zeolite-X which arises as a result of site heterogeneity, and which is unresolved in reversible isotherm measurements. These two states might correspond to sites present on the crystal surface and within the pore structure, respectively. Molecules in both state (1) and state (2) may undergo activated diffusion at appropriate temperatures.

With the present information we cannot determine which of these models is correct.

The diffusion activation energies measured in this work range from 2 to 3 kcal/mole. In Fig. 9 a schematic one-dimensional potential energy plot for a hydrocarbon molecule adsorbed at the surface or within the zeolite pores is shown. Once the molecule is adsorbed it has the choice of remaining as a surface species, desorbing into the gas phase, or diffusing into the zeolite crystal pores. As long as diffusion sites are available, it will choose to diffuse providing the temperature is sufficiently high.

It is instructive to calculate the steady-state *surface* coverage of 1-C_4H_8 during a typical adsorption experiment at 10^{-6} Torr. It is assumed that the sticking coefficient on the surface of a zeolite crystal is unity, and that only one migration jump leads to diffusion into the zeolite pore, where the molecule is then lost,

$$\text{arrival flux} = \frac{P}{(2\pi MRT)^{1/2}} = \text{departure flux} = \frac{N}{A}\nu_d e^{-E_d/RT} + \frac{N}{A}\nu_m e^{-E_m/RT}, \quad (2)$$

where P = pressure, N/A = steady-state coverage on crystal *surface*, E_d = activation energy for desorption, E_m = activation energy for diffusion, and $\nu_d = \nu_m \cong 10^{13}\ s^{-1}$.

If Eq. (2) is solved for $(N/A)_{ss}$, the steady-state 1-butene surface coverage, using E_d = 10.5 kcal/mole (*13*), we find for T = 225 K, and $P = 10^{-6}$ Torr that $(N/A)_{ss} = 1 \times 10^4/cm^2$; this coverage corresponds to a fractional surface coverage of 10^{-10}. The dominant term for depletion of the adsorbed layer in Eq. (2) is the diffusion term; however, even in the *absence* of diffusion into the bulk, under these conditions of temperature and pressure, for 1-butene the steady-state fractional surface coverage on the outside of the zeolite crystal will be very low.

This calculation demonstrates that for 1-butene the thermal desorption spectra should represent pore diffusion *exclusively* when the experimental temperature range is above 225 K. In contrast to this result, for C_2H_4 at 120 K where E_d = 8.9 kcal/mole, a *full monolayer* of C_2H_4 may be populated at 10^{-6} Torr, *assuming no depletion by diffusion*. This suggests that state (1) is probably representative of desorption of C_2H_4 from the *outer surface* of the zeolite crystallites.

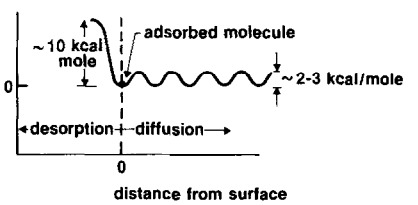

FIG. 9. Schematic one-dimensional potential energy diagram for a molecule at a zeolite surface.

C. *Adsorption and Diffusion Phenomena on a Zeolite Crystal*

In Fig. 10 we show a schematic representation of the depth profile of adsorbate concentration at various times and at a temperature where diffusion into the pore structure may occur. At time t_0, a steady-state pressure of adsorbate gas exists at the crystal face and, as shown by Eq. (2), a

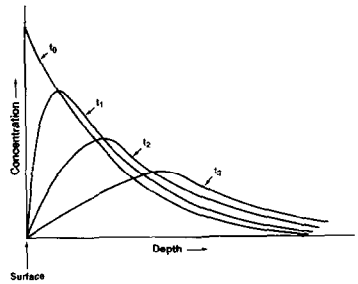

FIG. 10. Schematic representation of the evolution of adsorbate concentration profile within a zeolite crystal for various delay times following exposure. t_0: Adsorption occurring at zeolite surface; t_1–t_3: Increasing delay time under vacuum.

steady-state surface concentration exists, $(N/V)_{ss}$, accompanied by a diffusion profile into the crystal. We expect the developing concentration profile within the crystal to be described by $\text{erfc}[x/2(Dt)^{1/2}]$ which is the solution to Fick's law of diffusion into a semi-infinite one-dimensional continuum with a fixed concentration at the boundary. No second-layer diffusion occurs in this model. At time t_1, the gas phase has been pumped away and the steady-state surface concentration of adsorbate drops to near zero, since under vacuum the only supply of adsorbate at the crystal surface is by back diffusion from the pores. As time advances, adsorbate is lost by back diffusion followed by desorption and the maximum in the concentration profile advances in depth as forward diffusion occurs into the pore. For increasing delay times, the maximum in the thermal desorption spectrum will appear progressively later in time and thus the peak temperature will shift to higher temperatures as observed for 1-butene adsorbed at all temperatures and for C_2H_4 (state 2) adsorbed at $T \geq 190$ K. The time interval of the thermal desorption experiment itself may therefore be thought of as an extension of the delay period with the addition of a temperature ramp to accelerate the diffusion process. Because of the macroscopic depth involved in the zeolite pores, diffusion from the crystal is the slower process compared to desorption into vacuum once a molecule reaches the crystalline surface.

It is not our goal in this paper to present a rigorous mathematical model for these diffusion and desorption phenomena. Several such models involving various assumptions have been proposed and solved (*2, 8, 10*). On the basis of our results we can say that the approach employed by Chan and Anderson (*10*) seems the most realistic.

V. SUMMARY

Thermal desorption spectroscopy has been applied to the study of hydrocarbon adsorption on zeolite crystals using ultra-high-vacuum methods. It has been shown that this method possesses high sensitivity to detect at least 10^{-3}–10^{-4} of the saturation quantity of adsorbate, when zeolite samples of order 10^{-4} g in size are used. Samples of this size are useful in avoiding intergranular diffusion effects as well as temperature gradients expected for larger powdered samples.

It has been found that the thermal desorption spectroscopy method is able to discriminate absorbates present on the zeolite crystallite surfaces from adsorbates which have diffused into the zeolite pores. By adjusting temperature, exposure, and delay times at constant temperature following exposure, it is possible to study both the kinetics of desorption and of diffusion, and to obtain activation energies for both types of surface processes.

For zeolite-X, the activation energies for diffusion of C_2H_4 and 1-C_4H_8 have been estimated as 1.9 and 2.7 kcal/mole, respectively. The binding energy of adsorbed C_2H_4 on zeolite-X has been kinetically estimated to be 8.9 kcal/mole in excellent agreement with the isosteric heat of adsorption (8.9 kcal/mole) measured under equilibrium conditions.

ACKNOWLEDGMENTS

The authors acknowledge financial support for one of us (M.K.) from IREX (International Research and Exchange Board), and partial support from the De-

partment of Energy, Office of Basic Energy Sciences (J.T.Y.). We also acknowledge helpful comments from Dr. C. J. Powell, NBS.

REFERENCES

1. Yates, J. T., Jr., *Methods in Experimental Physics*, Academic Press, New York, N.Y. See also: (*a*) Menzel, D., *in* "Topics in Applied Physics—Interactions on Metal Surfaces" (R. Gomer, Ed.), Vol. 4, part 4. Springer-Verlag, Berlin, 1975. (*b*) King, D. A., *CRC Crit. Rev. Solid State Mater. Sci.* 7(3) (1978).
2. Cvetanovic, R. J., and Amenomiya, Y., *in* "Advances in Catalysis and Related Subjects," Vol. 17, p. 103. Academic Press, New York/London, 1967.
3. Barrer, R. M., Bultitude, F. W., and Sutherland, J. W., *Trans. Faraday Soc.* **53,** 111 (1957).
4. Bezus, A. G., Kiselev, A. V., Sedlacek, Z., and Du, P. Q., *J. Chem. Soc. Faraday Trans.* **67,** 468 (1971).
5. Rudham, R., and Stockwell, A., *in* "Catalysis—Vol. 1" (specialist Periodic Reports), (D. A. Dowden, Ed.), p. 87. The Chemical Society, London, 1977.
6. Rabo, J. A., Bezman, R. D., and Poutsma, M. L., *Acta Phys. Chem.* **24,** 39 (1978).
7. Barrer, R. M., and Sutherland, J. W., *Proc. Roy. Soc. Ser. A* **237,** 439 (1956).
8. Baranski, A., Ceckiewicz, S., and Caluszka, J., *Bull. Acad. Pol. Sci. Ser. Sci. Chim.* **24,** 645 (1976).
9. Iwamoto, M., Maruyama, K., Yamazoe, N., and Seiyama, T., *J. Phys. Chem.* **81,** 622 (1976).
10. Chan, Y.-C., and Anderson, R. B., *J. Catal.* **50,** 319 (1977).
11. King, D. A., Madey, T. E., and Yates, J. T., Jr., *J. Chem. Phys.* **55,** 3236 (1971); **55,** 3247 (1971).
12. Redhead, P. A., *Vacuum* **12,** 203 (1962).
13. Harlfinger, R., Hoppach, D., Hofman, H.-P., and Quitzsch, K., *Z. Phys. Chem. Leipzig* **260,** 905 (1979).
14. Doelle, H.-S., and Riekert, L., *in* "Molecular Sieves—II" (J. R. Katzer, Ed.), p. 401. ACS Symposium Series No. 40. Amer. Chem. Soc., Washington, D.C., 1977.